The Astrophysical Journal, 659:1702–1712, 2007 April 20

COOL-PLASMA JETS THAT ESCAPE INTO THE OUTER CORONA

Gianni Corti,[1] Giannina Poletto,[1] Steve T. Suess,[2] Ronald L. Moore,[2] and Alphonse C. Sterling[2]
Received 2006 December 4; accepted 2007 January 3

ABSTRACT

We report on observations acquired in 2003 May during a *SOHO-Ulysses* quadrature campaign. The UVCS slit was set normal to the radial of the Sun along the direction to *Ulysses* at 1.7 $R_\odot$, at a northern latitude of 14.5°. From May 25 to May 28, UVCS acquired spectra of several short-lived ejections that represent the extension at higher altitudes of recursive EIT jets, imaged in He II λ304. The jets were visible also in LASCO images and seem to propagate along the radial to *Ulysses*. UVCS spectra showed an unusually high emission in cool lines, lasting for about 10–25 minutes, with no evidence of hot plasma. Analysis of the cool line emission allowed us to infer the physical parameters (temperature, density, and outward velocity) of jet plasma and the evolution of these quantities as the jet crossed the UVCS slit. From these quantities, we estimated the energy needed to produce the jet. We also looked for any evidence of the events in the in situ data. We conclude by comparing our results with those of previous works on similar events and propose a scenario that accounts for the observed magnetic setting of the source of the jets and allows the jets to be magnetically driven.

Subject heading: Sun: corona

1. INTRODUCTION

There are a number of coronal transients that, although vaguely similar to coronal mass ejections (CMEs) in that material is ejected outwards, are not believed to be small-scale versions of those phenomena. Differences and similarities between "ejections" and CMEs are still indefinite. Ideally, such phenomena would be defined in terms of their respective driving mechanisms. These mechanisms, however, are not yet fully understood, and this is the crux of the problem.

About 5 yr ago, Gilbert et al. (2001) called attention to *narrow* CMEs—defined as CMEs whose apparent width is $\leq 15°$—that had been observed with the Large Angle and Spectrometric Coronagraph Experiment (LASCO; Brueckner et al. 1995) aboard the *Solar Heliospheric Observatory* (*SOHO*). According to the authors, narrow CMEs are not *jets* (because jets are said not to extend, usually, into the LASCO C3 field of view), but are phenomena whose limited spatial extent offers, with respect to larger scale events, a good opportunity for an unambiguous identification of their surface association. A spectroscopic study of some of these events has been made by Dobrzycka et al. (2003), who analyzed *SOHO* UVCS (Ultraviolet Coronagraph Spectrometer; Kohl et al. 1995) data and found temperatures and densities comparable to those of CMEs and slightly larger than those of polar coronal jets. Dobrzycka et al. concluded that their results could not give a definite answer to the question of whether narrow CMEs originate from expanding closed field structures or from reconnection with open field lines.

Bemporad et al. (2005) have recently studied recursive narrow ejections, dubbed "streamer puffs," which move out along a streamer without disrupting it. Visible in *SOHO* EIT (EUV Imaging Telescope; Delaboudinière et al. 1995), UVCS, and LASCO C2 and C3 coronagraphs, streamer puffs seem to originate from a compact explosion in the flank of a streamer, followed by the inflation of an outer loop of the arcade and subsequent reconnection events that unleash the "puff." Because only one of the narrow CMEs of Gilbert et al. (2001) and Dobrzycka et al. (2003) is streamer related, the Bemporad et al. (2005) phenomena constitute a class of events of their own, being neither a streamer blowout nor a jet rising up to a limited heliocentric distance.

Jets are enigmatic events, in that the word has been used in reference to different phenomena, from Hα surges to sprays and X-ray jets. The latter, for instance, observed by the Soft X-Ray Telescope (SXT) on *Yohkoh* (Tsuneta et al. 1991), are typically associated with bright point (BP) flares, active regions (ARs), or emerging flux regions (EFRs), and although their temperatures are typically $\geq 10^6$ K (and densities range between 10^8 and 10^{10} cm^{-3}), they may be associated with cool plasma, such as Hα surges (Shibata et al. 1992b). Shibata et al. (1992a) showed how a multidimensional magnetic structure in which reconnection occurs between emerging flux and a pre-existing oblique field may give rise to an ejection in which both hot and cool plasma coexist.

A multialtitude analysis of a jet occurring near a sigmoid AR has been recently presented by Ko et al. (2005), who studied the jet in *SOHO* CDS (Coronal Diagnostic Spectrometer; Harrison et al. 1995), EIT, UVCS, and LASCO, and in *TRACE* (*Transition Region and Coronal Explorer*; Handy et al. 1999) and Mauna Loa Solar Observatory data. This jet, observed both in cool (He I, H Lyα, C III) and hotter (Mg X) ions, never reached altitudes larger than 2 $R_\odot$, and its dynamics can be interpreted in terms of a ballistic model. Its physical properties comply with the reconnection-driven X-ray jet model.

There are, however, coronal white-light jets that have been observed in LASCO C2 and C3, both at the minimum and maximum of the solar activity cycle (at minimum they are localized in polar regions and referred to as "polar white-light jets"). These seem to originate from ARs in the vicinity of coronal hole (CH) edges or from small bipoles within CHs (Wang et al. 1998; Wang & Sheeley 2002). Their properties are similar to those of the jets previously described in that they are recursive phenomena that have a counterpart in *SOHO* EIT jets and travel almost ballistically. A previously unidentified property of jets has recently been pointed out by Wang et al. (2006), who analyzed a sample of 25 solar energetic particle (SEP) events and found that in ≈60% of the cases where EIT Fe XII images were

[1] INAF–Osservatorio Astrofisico di Arcetri, 50125 Firenze, Italy; corti@arcetri.astro.it, poletto@arcetri.astro.it.
[2] NASA Marshall Space Flight Center, Huntsville, AL 35812.

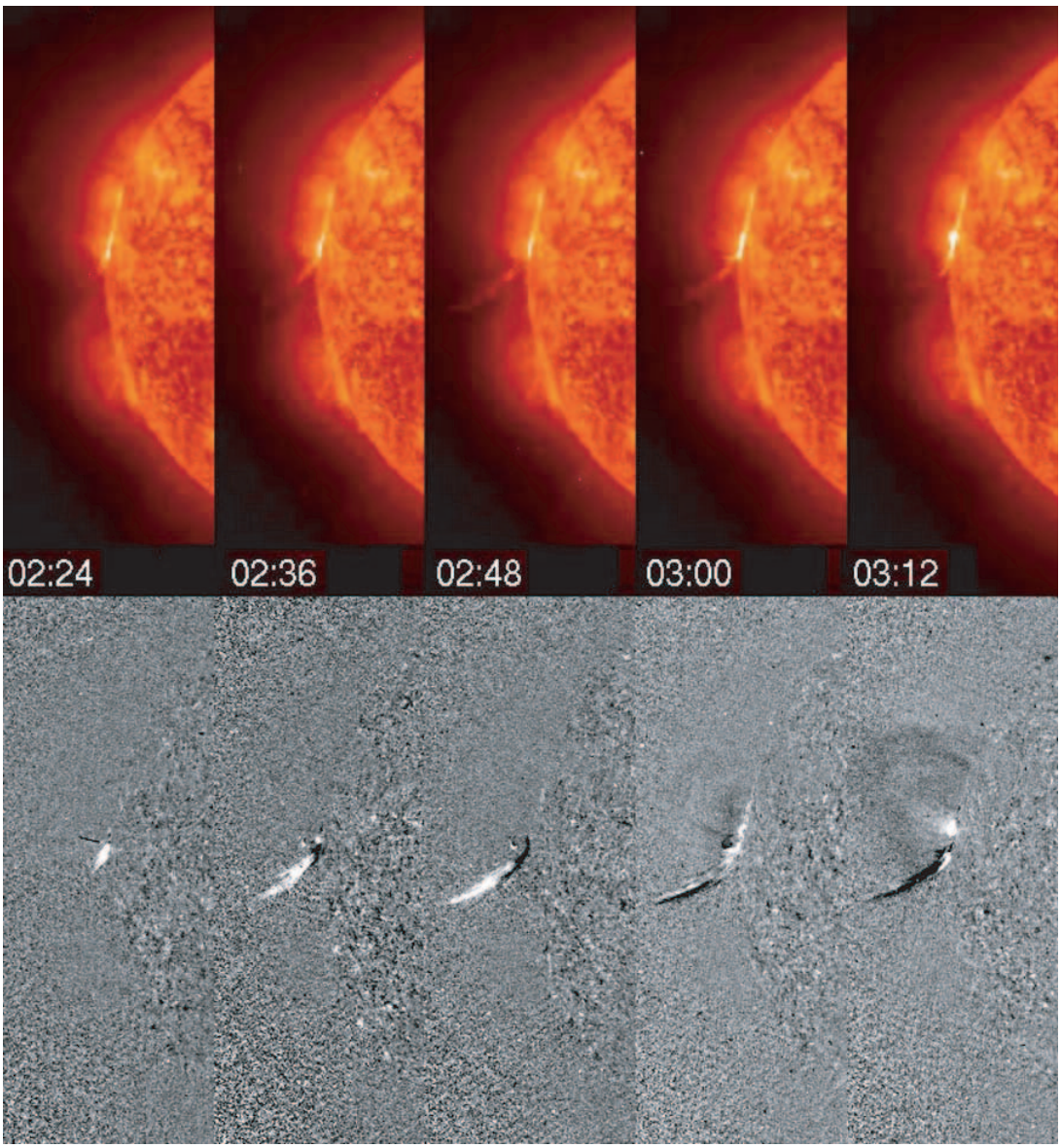

FIG. 1.—*Top*: EIT 304 Å images taken on 2003 May 27 showing the evolution of a jet, which projects above the northeast limb at a latitude of ≈5°. *Bottom*: EIT difference images, built from the images in the top row. This jet was last visible at 03:24 UT.

available, a Fe XII jet was associated with the SEP event. The authors surmise that, should EIT images be acquired at a higher temporal cadence, the percentage would be higher. The majority of the LASCO counterparts of the EIT/SEP events were narrow and fast.

That jets may be sources of energetic particles sheds light on their source mechanism. Reconnection within closed loops may in principle accelerate particles, but they would likely be trapped (Reames 2002). On the contrary, reconnection between open field lines and closed loops where, by footpoint exchange, plasma trapped within a loop is transferred to open field lines and ejected into the interplanetary medium, looks capable of explaining the jet/SEP association and fits the observed location of the white-light jets well (Pick et al. 2006).

In this work we contribute to a better knowledge of the jets by analyzing UVCS spectra of events that are the extension at higher altitudes (1.7 $R_\odot$) of recursive EIT jets. UVCS observations were acquired during the spring 2003 *SOHO*-Sun-*Ulysses* quadrature campaign, when jets that propagated along the direction of the radial to *Ulysses* were also imaged by the LASCO coronagraphs (see § 2). In § 2 we illustrate the scenario wherein the jets occurred, while in § 3 we examine UVCS spectra of the jets and give the temporal profile of their physical parameters. In § 4 we examine *Ulysses* data to check whether there is any evidence of coronal jets in the in situ data, and we discuss and summarize our results in the final section of this paper (§ 5).

2. THE OVERALL SCENARIO FOR THE 2003 MAY JETS

At the time of the spring 2003 quadrature, *Ulysses* was at a northern latitude of 14.5° in the eastern hemisphere at 4.91 AU. UVCS data were acquired over about 2 weeks around May 26, with the UVCS slit centered at the quadrature latitude and set normal to the radial to *Ulysses* at a heliocentric distance of 1.7 $R_\odot$. EIT started a CME watch campaign on May 26 that lasted through May 31, during which He II λ304 images were taken every ≈12 minutes. On May 26 and May 27 EIT observed a sequence of jets projecting above the solar limb around the quadrature latitude at a favorable position for the acquisition of

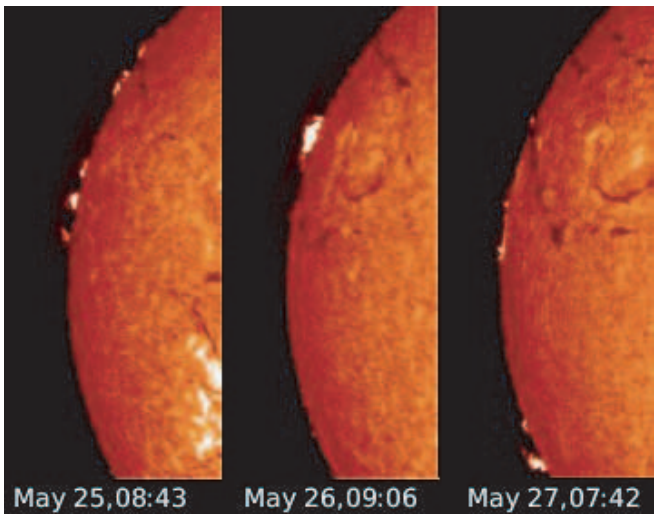

FIG. 2.—Hα images taken at the Kiepenheur Institute in Freiburg on (*from left*) 2003 May 25, 26, and 27, showing cool material above the limb, which projects at latitudes $\leq 20^{\circ}$ in the northeast quadrant.

UVCS spectra. Before illustrating UVCS data, we describe EIT, MDI, Hα, and LASCO data with the aim of understanding where the jets originated and the overall scenario that accompanied these events.

EIT images in He II λ304 detect upper chromosphere and transition region plasma at around 6×10^4 K. On May 26 and 27, these images showed frequent, recursive ejections, at a rate of about 10 events per day, emerging from the northeast limb of the Sun at a latitude of $\approx 5^{\circ}$ and rising until they disappeared from the EIT field of view. Individual jets appear in 1 to ≤ 5 images, which translates into typical lifetimes of a few minutes up to an hour. Short-lived activity may have been missed if it occurred in between the acquisition of successive images. Apparently, plasma rises upward along flux tubes that reach the outer boundary of the EIT field of view: during an event it is not unusual to see emitting material propagating outward along different flux tubes or emitted in spurts along the same flux tube or fanning out as in a sprinkler. The different morphology of different events and the 12 minute cadence of image acquisition makes any outflow speed determination uncertain; by associating a jet signature in UVCS (see § 3.1) with the brightest jet seen at lower levels by EIT, we have set its lower limit to ≈ 95 km s^{-1}. On May 28 the EIT events were still occurring, although as they projected onto the bright disk background their visibility greatly diminished.

Bright and long-lasting EIT jets occurred on May 26 at 16:36 and 18:00 UT and on May 27 at 02:36 and 06:24 UT. Figure 1 shows the May 27 jet, one of the longest lasting, observable over ≈ 60 minutes. We also show difference images in Figure 1, obtained by subtracting images taken 12 minutes apart. These help visualize changes due to flows of bright emitting material over the time span of the two images.

MDI (Michelson Doppler Imager; Scherrer et al. 1995) data show that NOAA AR 10373 rotated over the east limb early on May 28, being located at N08°, E67° at 23:00 UT of that day; this was the only AR in the northeast quadrant at that time. An Hα image taken by the Kiepenheur Institute in Freiburg shows in the early morning of May 27 the presence of Hα emitting material slightly southward of the quadrature angle (Fig. 2). Images taken on May 25 and 26 bear evidence of prominence material projecting slightly above the solar limb either side of that angle, proving that cool Hα material overlaid the AR.

We also examined LASCO images to check whether the EIT jets had reached up to the C2 and C3 coronagraphs' fields of view. Figure 3 shows LASCO C2 difference images for the event shown in Figure 1 and for a later event, still on May 27. The two events occur at the same position and show clearly that jets reach high coronal levels (and can be identified even in the C3 coronagraph). The presence of jets at the low coronal levels sampled by EIT and at the higher altitudes imaged by the C2 and C3 LASCO coronagraphs implies they may be detected at the intermediate UVCS altitudes.

3. UVCS OBSERVATIONS

The *SOHO* UVCS 2003 spring quadrature observations were aimed at the detection of CMEs and hence were made at a constant altitude (1.7 $R_{\odot}$), with the slit set normal to the radial to *Ulysses* at a latitude of 14.5°. The slit width was 100 μm, and the selected masks covered lines from ions originating in hot as well as in

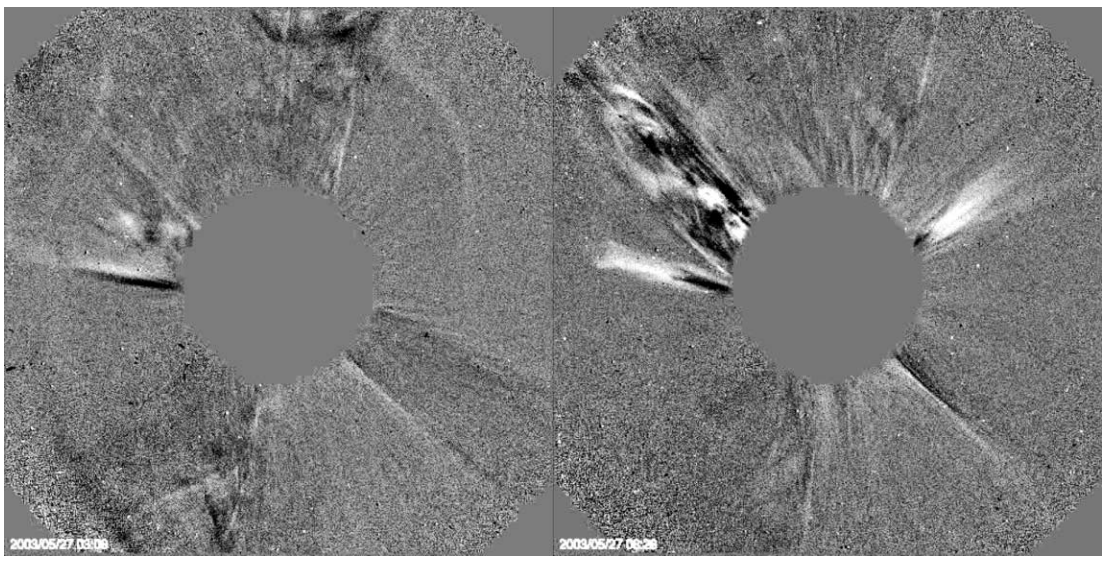

FIG. 3.—LASCO C2 difference images showing the jet shown in Fig. 1 at the time it reached the C2 field of view (*left*) and another jet, observed later (06:28) on May 27, at exactly the same position as the previous one (*right*).

TABLE 1
LINES IDENTIFIED IN THE UVCS SPECTRA OF JETS

Ion	Transition	λ_{obs} (Å)	log T_{max}
C III	$2s^2\ ^1S_0$–$2s\ 2p\ ^1P_1$	977.0	4.8
H I	Lyβ	1025.7	4.5
O VI	$1s^2\ 2s\ ^2S_{1/2}$–$1s^2\ 2p\ ^2P_{3/2}$	1031.9	5.5
O VI	$1s^2\ 2s\ ^2S_{1/2}$–$1s^2\ 2p\ ^2P_{1/2}$	1037.6	5.5
H I	Lyα	1215.7	4.5

cooler plasma. Different masks were used on May 26 and 27. On May 26 the detector masks binned the data over 6 pixels (42″) in the spatial direction; data have a 2 pixel spectral binning (0.1986 Å bin^{-1}) in the 1023.97–1043.23, 967–981, 1005–1013, and 998–1002 Å wave bands, and a 3 pixel spectral binning (0.2979 Å bin^{-1}) in the 943–966 and 1170–1191 Å spectral intervals (the latter imaged in the "redundant" channel). On May 27 the detector masks binned the data over 5 pixels (35″) in the spatial direction; data have a 1 pixel spectral binning (0.094 Å bin^{-1}) in the 1022.2–1043 Å wave band and a 2 pixel spectral binning in the 974.5–988, 1210–1222, and 996–1001 Å wave bands. The 1210–1222 Å band is seen in the redundant channel and covers the H Lyα line. The raw data have been wavelength and flux calibrated; stray light appears to be negligible and there was no need for stray-light corrections.

On May 26, UVCS data were acquired after 16:52 UT when a LASCO CME, at 16:50 UT, had probably already gone through the 1.7 $R_\odot$ altitude where the UVCS slit was set. However, we surprisingly found no evidence of this or of later LASCO CMEs. Analogously, on May 27 UVCS data were acquired from 00:38 to 02:49 UT and from 06:50 to 16:50 UT, which were periods without LASCO CMEs. The reason UVCS did not detect any CME plasma lies in the source region of the CMEs: EIT images show clearly that they originated in AR 10365, which was at the disk center (S08°, W06°) on May 26. Hence, the CME plasma was much farther from the Sun than the 1.7 $R_\odot$ where UVCS would have observed it, if laying in the plane of the sky.

We then searched the UVCS spectra looking for signatures of the He II jets and detected two events: one on May 26, starting at ≈19:34 UT, and a second on May 27, which was already in progress when we started our observing campaign at 06:50 UT. The distinctive signature of these events is their emission in the C III λ977 line, which is not visible in coronal spectra, as the temperature of maximum C III ion formation is 6.3×10^4 K. Jets are observed in neutral hydrogen lines, such as Lyα and/or Lyβ, and/or in the O VI doublet lines at 1032, 1037 Å. There was no jet emission from hotter lines, such as [Si VIII] λ944, [Fe X] λ1028, or Si XII λ499 (observable in the second order), which require plasmas at $T \geq 5 \times 10^5$ K. Table 1 gives the lines detected in jets, with the temperature of maximum formation of the emitting ions. The lines have no Doppler shift; hence, the emitting features lie in the plane of the sky.

3.1. *The May 26 Jet: Morphology and Physical Parameters*

The UVCS jet of May 26 first appeared in EIT at 18:00 UT. Figure 4 is a composite image showing the EIT He II image, the position of the UVCS slit, and the LASCO image where the continuation of the jet at higher altitudes is easily identified. The event is composed of at least two jets: Figure 5 shows the first three EIT images in which the jets were observed. Only one of these was detected by UVCS. Assuming it was ejected at an intermediate time in between the acquisition of two successive EIT images, a crude evaluation of its speed between the limb of the Sun and the altitude where it was observed by UVCS gives $v_{out} \approx 95$ km s^{-1}, with an uncertainty of ±5 km s^{-1}. The jet appeared in LASCO images at 19:50 UT; because LASCO images are acquired every ≈24 minutes, the time when the jet first entered the LASCO field of view is also not well defined. A crude evaluation of the speed of the jet in between the UVCS and LASCO levels gives a lower limit to the speed of $v_{out} \approx 350$ km s^{-1}. This means that the jet is accelerating with altitude.

Figure 6 gives the temporal evolution of the C III λ977, O VI λ1032, and H Lyβ intensity along the UVCS slit, for the May 26 event. Units along the horizontal axis are minutes, starting at t = 18:51 UT. The jet emission lasts about 10 minutes; during

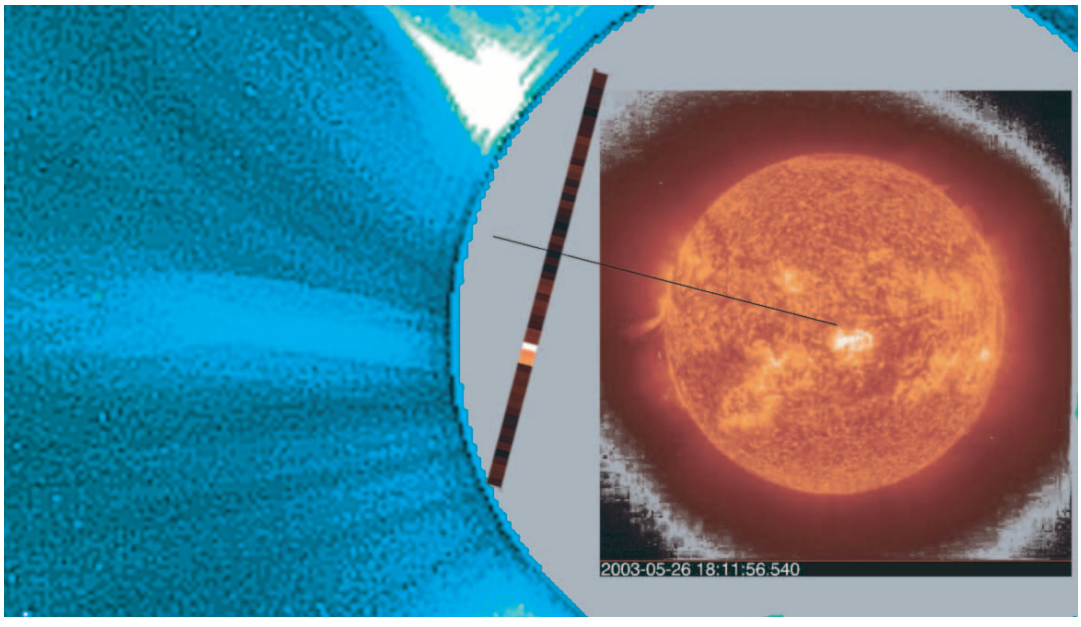

FIG. 4.—Composite image showing the jet of 2003 May 26 in the low corona in the EIT He II image acquired at 18:12 UT; as a bright spot along the UVCS slit, at 1.7 $R_\odot$ and 19:40 UT (UVCS slit width not to scale), and at higher levels in a LASCO C2 image at 20:06 UT.

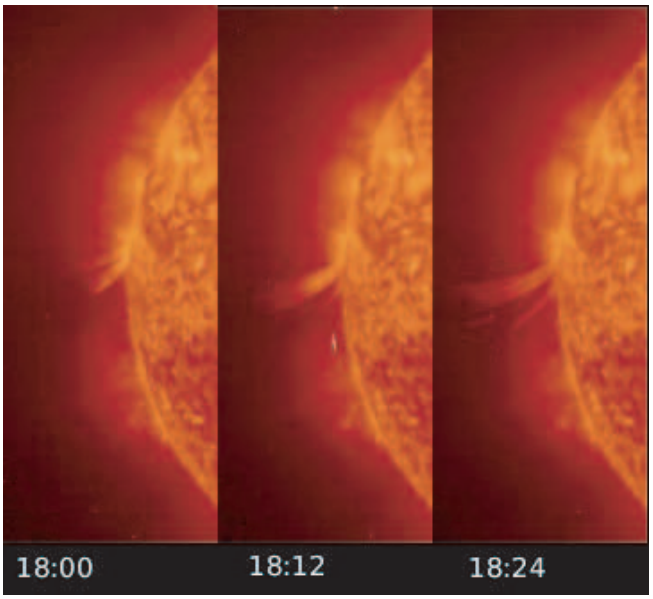

FIG. 5.—May 26 jet in three successive images in the EIT He II λ304 filter.

the jet passage through the slit the C III line intensity increases by more than a factor 10 above the background noise. The C III and O VI lines appear simultaneously in the UVCS field of view; the H Lyβ line is hardly identifiable over the background level, although probably going through a small increase during the jet transit.

In typical coronal conditions (low electron density and high electron temperature) spectral lines form by electron collisional excitation followed by spontaneous emission. In this case, the line emissivity $\epsilon_{\rm line}$ can be defined as

$$\epsilon_{\rm line} = A_{\rm el}\frac{n_{\rm ion}}{n_{\rm el}}(T_e)B_{\rm line}q_{\rm line}(T_e)\ \text{photons cm}^3\ \text{s}^{-1}, \quad (1)$$

where $A_{\rm el} = n_{\rm el}/n_{\rm H}$ is the absolute abundance (i.e., relative to hydrogen) of the element whose ion has an ionic fraction $n_{\rm ion}/n_{\rm el}$ (which is a function of the electron temperature T_e) and $q_{\rm line}(T_e)$, $B_{\rm line}$ are, respectively, the electron excitation rate and the branching ratio for the line transition. The line intensity is related to emissivity by

$$I_{\rm coll} = \frac{1}{4\pi}\int_{\rm LOS}\epsilon_{\rm line}n_e n_{\rm H}dl\ \text{photons cm}^{-2}\ \text{s}^{-1}\ \text{sr}^{-1}, \quad (2)$$

where n_e, $n_{\rm H}$ are, respectively, the electron and proton densities (cm^{-3}) and the integration is along the line of sight (LOS).

However, coronal lines that also have a strong chromospheric component are formed both by collisional and radiative excitation: this is certainly the case for the C III, H, and O VI lines in which the jet shows up. The radiative emission of a line depends on the electron temperature, the electron density, the intensity of the exciting chromospheric radiation, and on the plasma outflow speed.

A concise expression for the intensity of the resonantly scattered component of a line in an isothermal plasma flowing outward at a speed v is

$$I_{\rm rad} = \text{const}\,A_{\rm el}\langle D(v)\rangle\frac{n_{\rm ion}}{n_{\rm el}}\int_{\rm LOS}n_e dl\ \text{photons cm}^{-2}\ \text{s}^{-1}\ \text{sr}^{-1}, \quad (3)$$

where $D(v)$ is the Doppler dimming term that can be expressed as

$$D(v) = \int_0^\infty I_{\rm disk}\Phi(\lambda-\lambda_0)d\lambda; \quad (4)$$

here $I_{\rm disk}$ is the exciting chromospheric radiation, Φ is the normalized coronal absorption profile that depends on v and λ, and λ_0 is the wavelength at the line center (see, e.g., Li et al. [1998] for an expanded expression of $I_{\rm rad}$).

$D(v)$ is a crucial parameter because, depending on how fast the ion is moving, the exciting chromospheric radiation is Doppler shifted in the ion frame of reference and becomes unable to radiatively excite the line, whose radiative component may thus vanish. Figure 7 gives the C III λ977 Doppler dimming curve, showing the percentage decrease in the radiative line intensity as a function of the outflow speed v of the emitting ion, normalized to the intensity in a plasma at rest.

Because the *average* speed of the jet between the limb of the Sun and the 1.7 $R_\odot$ altitude of the UVCS slit is on the order of

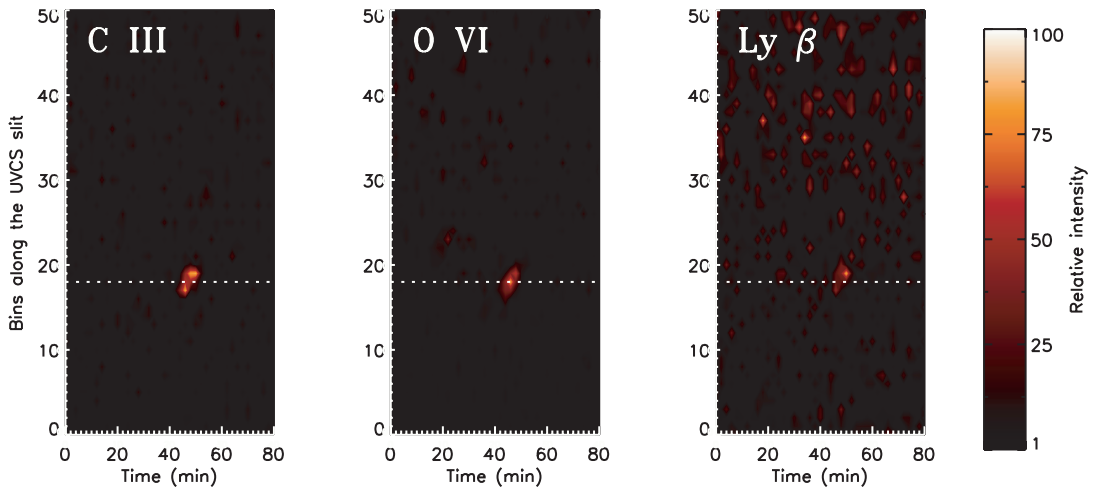

FIG. 6.—Time profile of the May 26 jet, as observed by the UVCS spectrograph in the C III λ977, O VI λ1032, and H Lyβ lines. Positions along the slit are given in the vertical axis: the radial to *Ulysses* cuts across the slit at bin 32. Times are given along the horizontal axis, starting from 18:51 UT. The figure gives the line intensities in photons s^{-1} cm^{-2} sr^{-1}, integrated over the spectral width of the line after subtracting the prejet coronal emission.

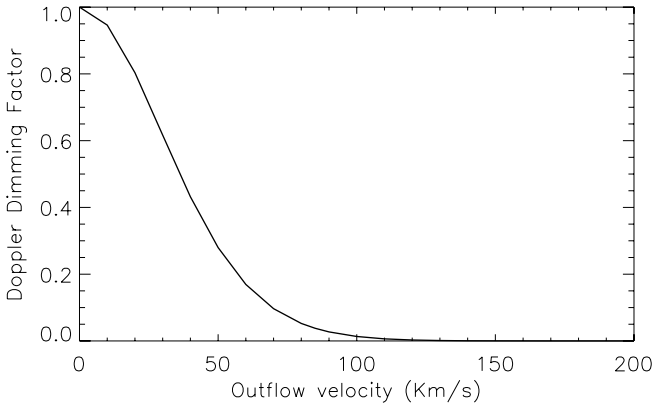

FIG. 7.—Doppler dimming factor for the C III λ977 radiative emission: for an outflow speed of 100 km s^{-1} the line emission is reduced to about 2% of the emission in a plasma at rest.

95 km s^{-1}, we can safely assume that the radiative component of the line has been completely Doppler dimmed and that the line, at the altitude of the UVCS slit, forms exclusively by collisional excitation (eq. [2]). This also holds true for the O VI λ1032 line, and so its intensity is also given by equation (2). Hence, the ratio of the intensities of the C III and O VI lines depends only on the electron temperature, and assuming the lines form in a plasma with photospheric abundances (Feldman et al. 1992), it can be easily evaluated. Once the electron temperature has been identified, the plasma emission measure $\int_{\rm LOS} n_e n_{\rm H} dl$ and its electron density (assuming the jet has a cylindrical shape) are derived from equation (2). With this technique we evaluated T_e, n_e in the jet over the time it was observed by UVCS.

The Lyβ line, on the contrary, due to its large chromospheric radiation has both a collisional and a radiative component; the latter contributes to the line intensity at outflow speeds for which the C III and O VI radiative intensity is negligible. Equations (3) and (4) show that by calculating the total H Lyβ intensity with the density and electron temperatures previously derived from the ratio of the C III and O VI lines we can determine the value of $D(v)$, hence the outflow speed for which the radiative component, added to the collisional component, reproduces the observed intensity. Table 2 summarizes the physical parameters of the May 26 jet over the time it was observed by UVCS.

Table 2 shows that, unfortunately, the outflow speed of plasma can only be crudely constrained. Initially, the Lyβ signal is indistinguishable from the background noise and also in the three successive spectra has such a low intensity (hence large statistical errors) that we chose to fit only the Lyβ intensity summed over the three spectra. All speed values within the interval given in Table 2 reproduce the Lyβ intensity with an 8% accuracy, because the Lyβ dimming curve is relatively flat over that interval of speeds. The absence of other lines does not allow us to put better constraints on the jet parameters.

TABLE 2

PHYSICAL PARAMETERS OF THE 2003 MAY 26 JET FROM SPECTROSCOPIC ANALYSIS

Observation Time (UT)	T_e (K)	N_e (cm^{-3})	$v_{\rm out}$ (km s^{-1})
19:38:45	1.8E5	8.7E6	$\geq$110
19:40:55	1.8E5	1.3E7	150–220
19:43:04	1.7E5	1.2E7	150–220
19:45:15	1.7E5	8.3E6	150–220

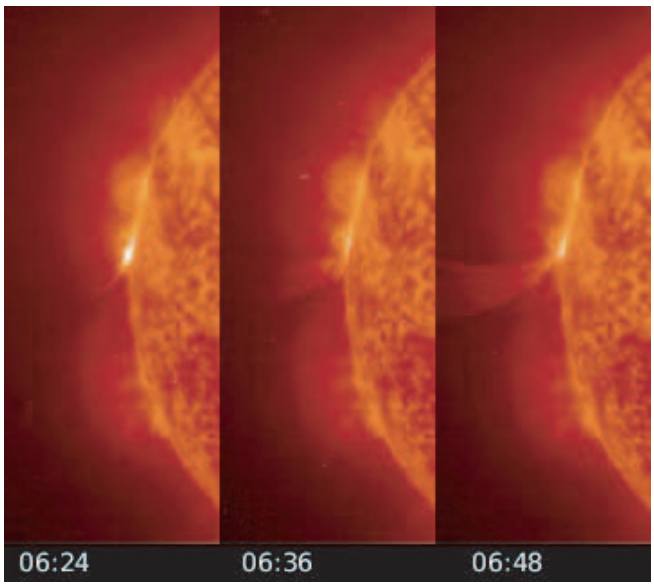

FIG. 8.—May 27 jet in three successive images in the EIT He II λ304 filter.

Tentatively, we conclude that over the time spent at 1.7 $R_\odot$ the jet has a constant temperature $T_e = 1.75 \times 10^5$ K ($\pm 0.5 \times 10^4$ K) and density $n_e = 1.05 \times 10^7$ cm^{-3} ($\pm 0.22 \times 10^7$). Possibly, the density initially reaches a plateau through a 35% increase and falls back to its initial value through an analogous decrease before disappearing from the UVCS field of view. We expect to derive a more precise picture of the jet parameters and of their temporal evolution from the spectra of the May 27 jet, where we observe the Lyα line, which forms by radiative excitation only and is much stronger than the Lyβ line.

3.2. *The May 27 Jet: Morphology and Physical Parameters*

Figure 8 shows three successive EIT images in which the May 27 jet was observed. Because the jet was in progress at the time (06:50 UT) UVCS started its observations, we cannot make an estimate of its speed as we did for the May 26 event, and we have to rely on the lower limit of $\approx$95 km s^{-1} mentioned in § 2. An evaluation of the speed of the jet at 03:24 UT on 2003 May 27 (Fig. 1) leads to a value of $\approx$128 km s^{-1}, supporting our assumption of an ejection speed $\geq$95 km s^{-1} for the jets we are analyzing.

The jet was observed by UVCS in the H Lyα and Lyβ and in the C III and O VI lines. The jet position does not coincide with that of the May 26 jet, although the source region is obviously the same. Moreover, over its lifetime, the jet seems to shift slightly in position. This behavior is clearly visible in Figure 9, which shows the event to consist of three jets in part superposed in time, to be interpreted as a subsequent brightening of close-by loops or as the successive brightening of the same structure.

Before applying the procedure used for the determination of the physical parameters of § 3.1, we have to identify which percentage of the total line intensity has to be ascribed to each jet. To this end, whenever there is a partial superposition in the spatial position of two emitting jets, we fit the spatial distribution of the intensity of the strongest emitting jet with a Gaussian and ascribed the difference between the observed and the Gaussian distribution to the emission of the second jet. The technique has been applied to establish the percentage C III and H Lyα emission of the first and second jet in a time sequence whenever their spatial shift allowed an unambiguous separation of the two emitting

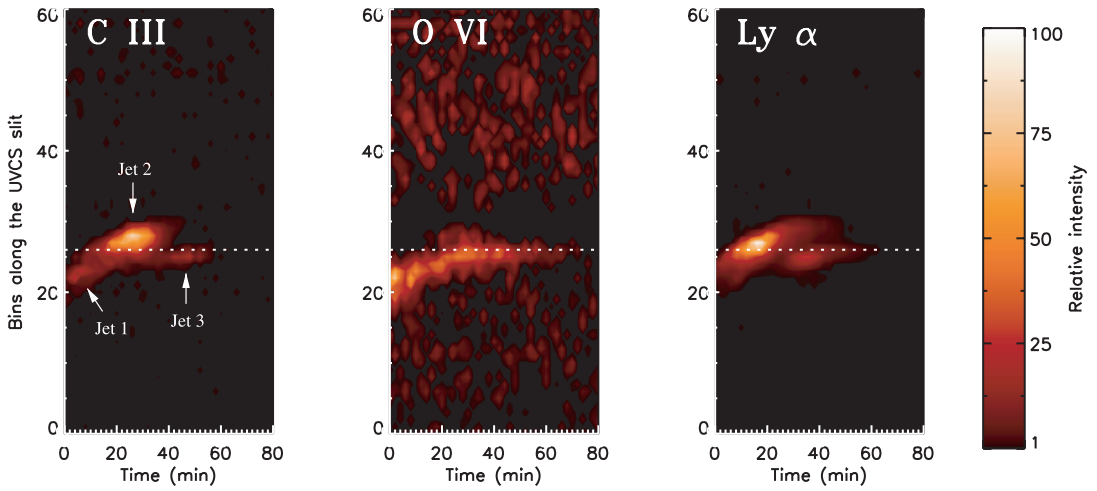

FIG. 9.—Isocontours of the C III λ977 intensity (*left*), the O VI λ1032 intensity (*middle*), and H Lyα intensity (*right*) as a function of time along the UVCS slit for the May 27 jet.

components. We point out that the second jet does not emit in the O VI λ1032 line, as it occurs at a spatial position where the O VI emission is at the background level. Because the third jet starts when the first has already faded, its O VI emission is well defined and there is no ambiguity in assigning the O VI emission to one jet or the other (see Fig. 9).

Figure 10 gives an example of the Gaussian fitting of the spatial distribution of the C III λ977 intensity at $t = 07{:}14{:}01$ UT (11th exposure): the asymmetric "bulge" has been ascribed to the emission of the weaker emitting jet (jet 1 in Fig. 9). Figure 11 shows the temporal profile in the C III λ977 and in the H Lyα line emission of the three jets, as inferred after identifying the components emitted in individual events.

These reconstructed C III and H Lyα intensities and the measured O VI intensities constitute the set of data for the three jets on 2003 May 27, which we use to constrain the physical parameters of the three events. In our scenario, the first and third jet (analogously to the May 26 event) show emission in the O VI λ1032 line, while the second jet emits only in C and H lines. Qualitatively, this means that the second jet has a lower temperature than the others.

Because the UVCS grating position adopted on May 27 allowed us to observe the strongly emitting H Lyα line, the physical parameters of the May 27 first and third jet can be precisely

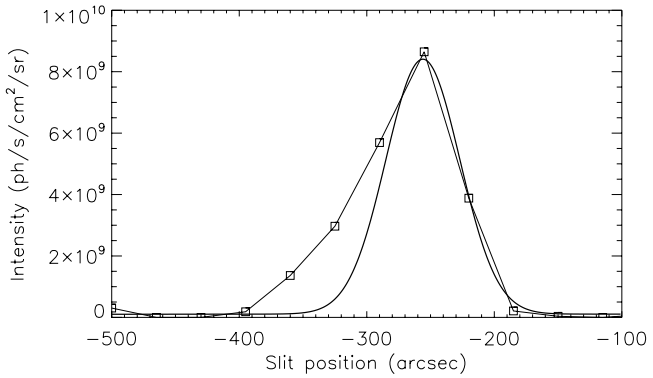

FIG. 10.—Gaussian fit of the spatial distribution of the strongest component of the C III emission from two jets on 2003 May 27, 07:14 UT. Positions along the UVCS slit are given in the abscissa.

identified. Assuming, as we did before, that the C III and O VI lines are collisionally excited, we derived the electron temperatures and densities that reproduce the observed line intensities and then inferred the plasma outflow speed that reproduces the intensity of the radiatively emitted Lyα line.

Results for jet 1 are given in the left panel of Figure 12. The observed intensities are reproduced, with the parameters shown in the figure, within an 8% accuracy. As in the May 26 event, the jet had a constant temperature $T_e = 1.70 \times 10^5$ K with fluctuations of 6×10^3 K over the time it was observed by UVCS. The jet speed decreases by no more than ≈25% over about 22 minutes, while the density declines steadily and has decreased by ≈37% of its maximum value at the time it is last seen by UVCS. Jet 1 was in progress at the time UVCS started its observations: hence we cannot say anything about the initial phase of the jet. However, we may be able to see the initiation of jet 3 (see Fig. 9), which we interpreted as an injection of O VI emitting plasma in the same flux tube where jet 1 occurred.

Figure 12 (*right*) shows the temporal profile of T_e, n_e and of the outflow speed of jet 3. The temperature turns out to be $T_e = 1.68 \times 10^5$ K with fluctuations of 6×10^3 K over the time it was observed by UVCS, and the density falls to about 50% of its maximum value at the end of the event. The outflow speed of the jet appears to increase initially; this behavior may not have been observed in other episodes either because of their duration, too short with respect to the time integration of data (see the May 26 jet), or because data at the beginning of the event had not been acquired (see May 27, jet 1). Unfortunately, even if the C III emission of jet 3, at the start of the event, has been derived by disentangling the jet 2 and jet 3 components from the observed overall intensity, the C III intensity is about 1 order of magnitude lower than the jet 2 emission; hence its identification is subject to large errors. We conclude that these data do not allow us to draw firm conclusions on the early behavior of jets.

As we pointed out earlier, jet 2 has the lowest temperature of all the jets, because it has no emission in the O VI line. This makes the identification of the physical parameter of the jet more ambiguous, as we have to rely on a line that only forms collisionally (C III λ977), on H Lyα, which forms only radiatively, and on H Lyβ, which has both a collisional and a radiative component, but has a much lower intensity than the other lines and originates from the same ion as one of the other lines (hence has the same

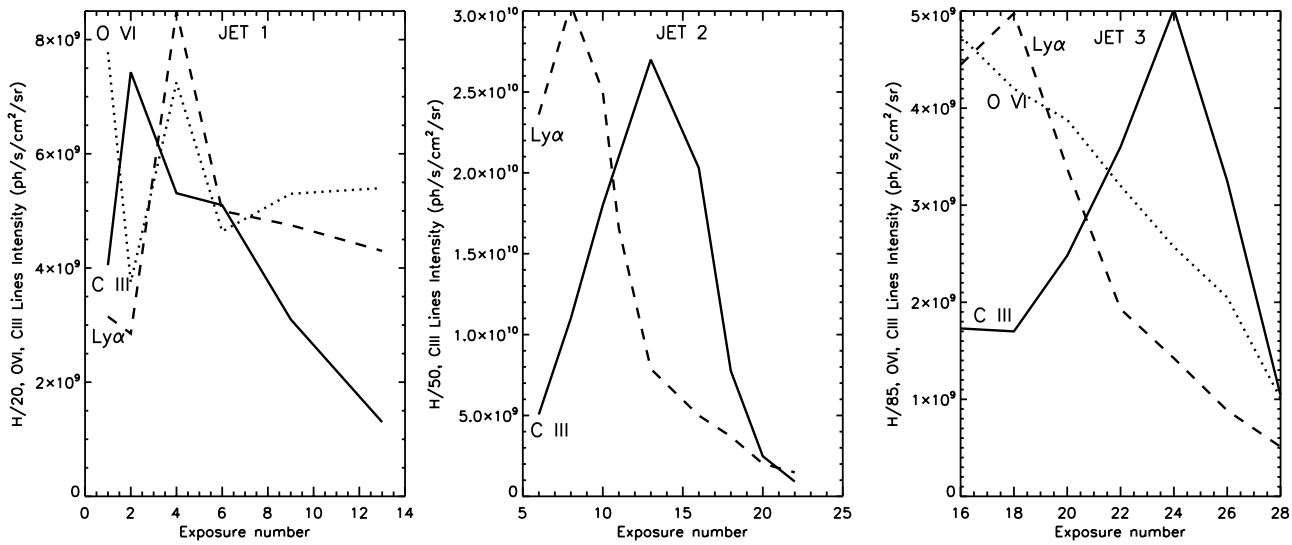

FIG. 11.—Reconstructed profiles of the C III λ977 (*solid lines*), H Lyα (*dashed lines*), and O VI λ1032 (*dotted lines*) intensities vs. time during the evolution of the first, second, and third jets. Intensities have been reconstructed with the technique illustrated in the text when emission from different jets was spatially superposed.

temperature dependence). In this case, we had to resort to an a priori further constraint to be able to derive the jet physical parameter. Because it seems well established from the other events that jets are isothermal throughout the time they are observed by UVCS, we first chose to search for densities and speeds, which, keeping T_e constant, allow us to reproduce the line intensities. To this end, from the collisionally excited C III line we derived the plasma density as a function of the a priori selected temperature and found pairs of T_e, n_e values for which lines could be reproduced within 10% of the observed values. Results from this procedure are given in Figure 12 (*middle*). The inferred temporal profiles of the density and outflow speed of jet 2 are consistent with the behavior found in the other jets, with an initial increase in the speed and a rapid decline in density when the jet is last observed. Jet densities are on the order of densities in streamers, at the same heliocentric distance (see, e.g., Gibson et al. 1999) and a factor $\approx$50 higher than typical densities in coronal holes (see, e.g., Guhathakurta et al. 1999).

4. *ULYSSES* OBSERVATIONS

Detecting these small jets at *Ulysses* is potentially possible, even though *Ulysses* was at 4.91 AU. Some of the jets appear to move out approximately along the radial direction to *Ulysses* in LASCO C2. Previously, we reported an equally small transient at comparable large distance (Suess et al. 2000). However, that transient was embedded in a long interval of exceptionally smooth slow solar wind. In the present case, the jets are embedded in an interval of numerous small CMEs that was surrounded by large CMEs on May 26, and June 1 and 2 (see § 2). This severely limited the detectability of the jets.

Ulysses data were searched for several days around the expected arrival time of the jets, approximately 2 weeks after they

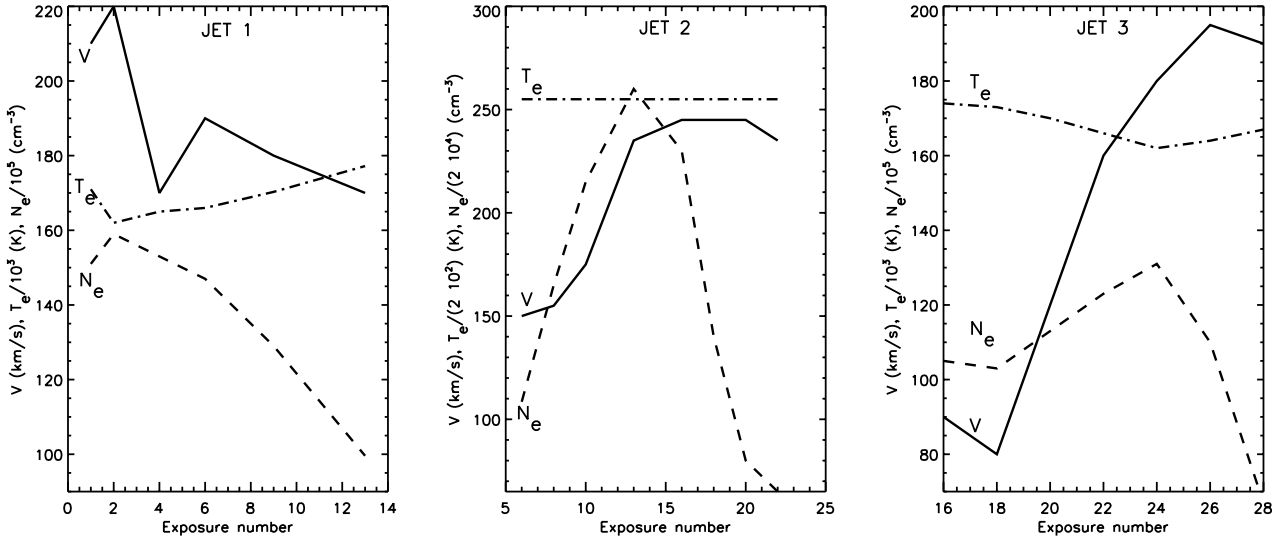

FIG. 12.—Electron temperature (*dot-dashed lines*), electron density (*dashed lines*), and outflow speed (*solid lines*) during the lifetime of the jet first observed on 2003 May 27, 06:50 UT (exposure 0; *left*); the jet that started on 2003 May 27, at 07:01 UT (exposure 5; *middle*), for which the temperature has been assumed to remain constant throughout the jet lifetime; and the jet that started on 2003 May 27, at 07:25 UT (*right*). Exposures are taken every $\approx$120 s.

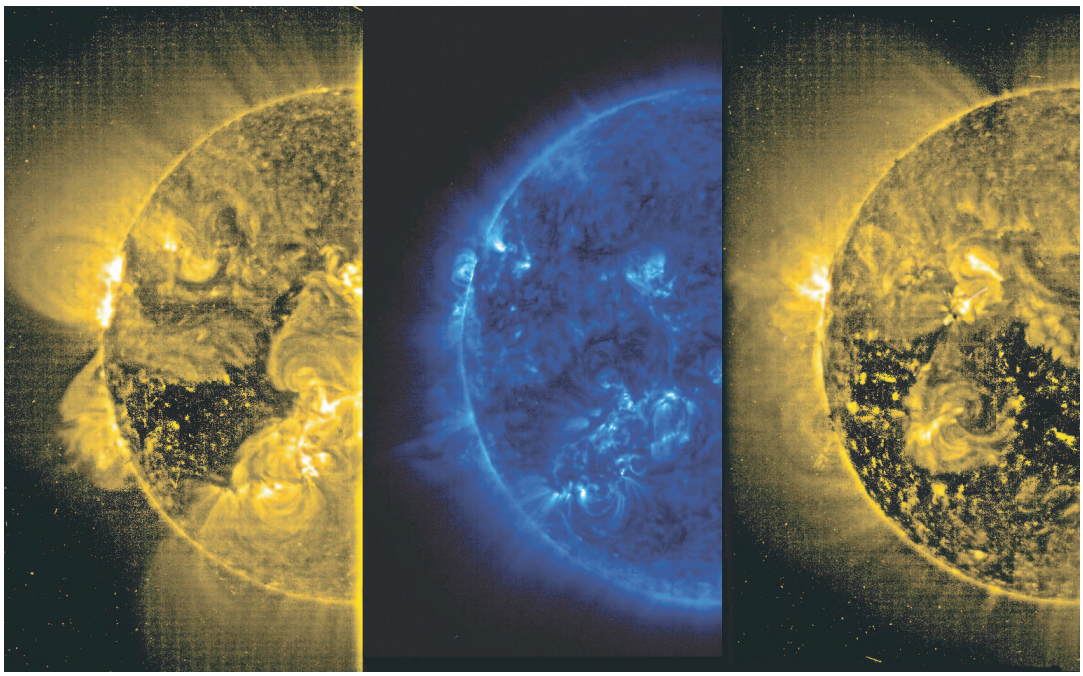

FIG. 13.—*Left and right*: Disk images in EIT Fe XV λ284 on, respectively, 2003 May 26 and 2003 May 31. The images show that AR 10373, where jets originated, lies at the edge of a large CH area void of emission (except for a small bright emitting region south of 10373). *Middle*: Disk images in EIT Fe IX/X λ171 on 2003 May 26, showing the quadrupolar configuration of AR 10373, where two systems of loops join opposite polarities and are surmounted by a higher arcade linking the outer AR edges is clearly visible in the May 26 image, when the AR is at the limb of the Sun.

were observed at the Sun. Interplanetary CMEs (ICMEs) have several typical signatures, including enhanced alpha particle abundances and elevated Fe charge state (Bemporad et al. 2006), and the large CMEs on May 26 and June 1, 2 were easily identified. No obvious signature was seen from the jets, while the expected location of the jet ejecta could be isolated to within an interval of about 2 days between the ICMEs. A lack of evidence of enhanced Fe charge state might be expected due to the low temperatures in the jets. So, we also searched in relatively cool ions: Si X, C VII, and Ne IX, for which there were also no obvious enhancements. The conclusion is that the jets either had no signature in cool ions or were indistinguishable from the surrounding ambient slow solar wind in which they were embedded.

Ulysses may have detected the reconnection event that may have been responsible for the jets, in terms of the resulting type III radio bursts. A large number of type III bursts were seen with the radio wave experiment (URAP) on May 26–27. The largest of these events coincide with the times the He II jets were first seen in EIT. Type III bursts are caused by relativistic electrons traveling out along the spiral interplanetary magnetic field. *Ulysses* energetic particle data (HI-SCALE) were checked for evidence of the relativistic electrons causing these bursts, but none was seen. This could be a result of *Ulysses* not being at the correct longitude to intersect the spiral originating at the source (Pick et al. 2006).

5. DISCUSSION AND CONCLUSIONS

Summarizing the results we obtained for the physical parameters of jets observed at 1.7 $R_\odot$ we conclude that

1. Jets have a constant temperature over their lifetime, but may have different temperatures in different events. Those we analyzed are "cool" events: the highest temperature they reach is $\approx 1.7 \times 10^5$ K and their plasma is strictly isothermal, with an uncertainty of $\approx (5-6) \times 10^3$ K.

2. Jets disappear because their density substantially decreases at the trailing end, as if the material being hurled outward is exhausted or the force that ejects the material turns off.

3. The total mass in the jets, estimated from their density, speed, and duration at 1.7 $R_\odot$ turns out to be on the order of 10^{13} g, on the low side of CME masses but well above the 10^{11} g threshold for detection with LASCO coronagraphs.

4. We are unable to describe in detail the behavior of the jet speed; possibly, it increases at the start of the event, but it appears not to decrease in its final stages.

From EIT He II observations we know that there are many such events on May 26 and 27, and that the AR where they originate keeps showing this transient activity as it rotates past the limb of the Sun, at least on May 28, although jets become much less evident as they project onto the bright disk background. Later on, they may eventually disappear. EIT images in Figure 13 show that the AR where jets occur comprises two bipolar regions, surmounted by an arcade connecting the region outer boundaries. Comparison of Figure 13 (*left and right*) with full-disk He II images at the times of jets demonstrates that jets originate from the southernmost edge of the AR and extend into a dark area where open fieldlines are rooted. This is further supported by the potential field source surface (PFSS) extrapolation (see Fig. 14) of the National Solar Observatory (NSO) photospheric field for Carrington rotation 2003, which shows the field line configuration of 2006 May (*left*) and at a time when the east limb is at the central meridian (*right*).

This makes the magnetic configuration where jets originate similar to that in which the Wang & Sheeley (2002) and Wang et al. (2006) jets occurred, and we analogously surmise that the 2003 May jets are produced by reconnection of closed loops in AR 10373 with adjacent open field lines. As ejections occur at the limb of the Sun, we cannot see what triggers reconnection: most likely an emerging included polarity at the southern edge

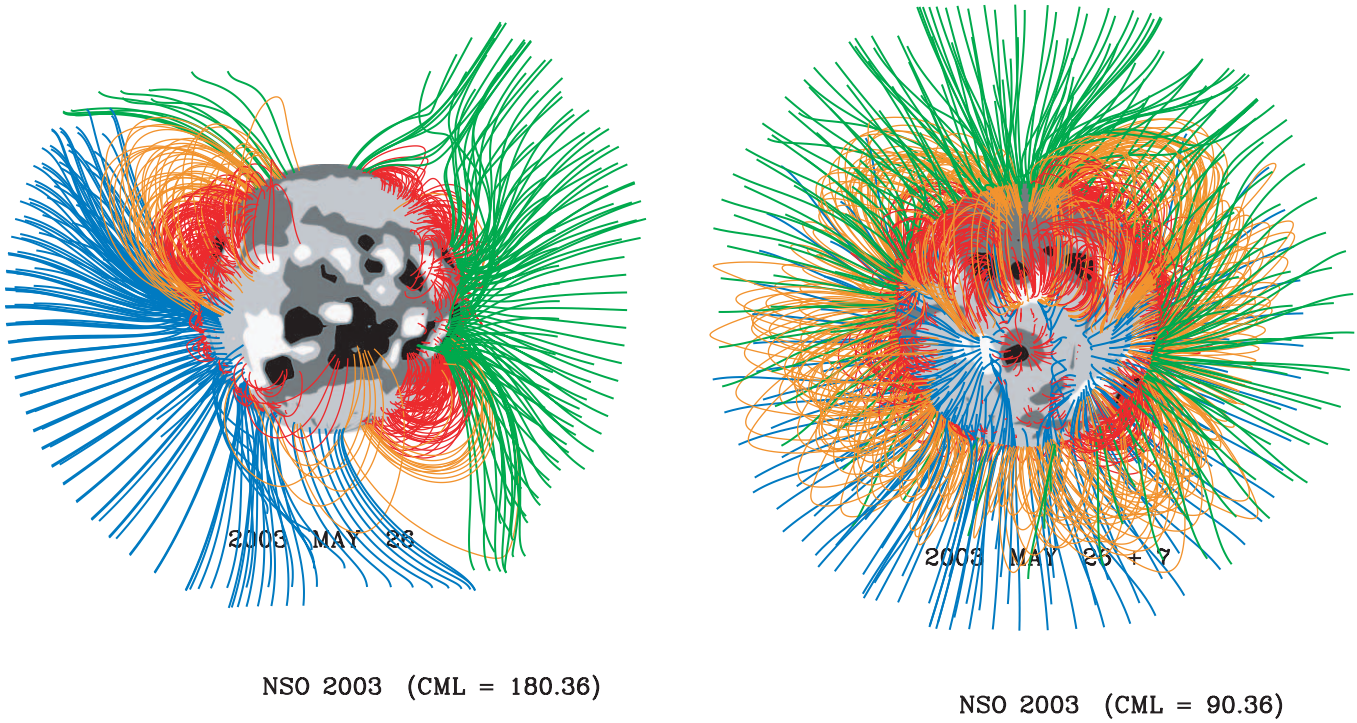

FIG. 14.— Potential field line extrapolations from the NSO photospheric field of Carrington rotation 2003. *Left*: Field line configuration for 2003 May 26. *Right*: Field structures after a 90° rotation when the May 26 east limb is at the central meridian. Open field lines are shown in blue (courtesy of Yi-Ming Wang).

of the AR. This is shown to occur in one of the Wang et al. (2006) jets (see their Fig. 13). On May 31, when AR 10373 is closer to disk center, flux emergence at the place where jets had been occurring is clearly seen on MDI magnetograms.

The cartoon in Figure 15 gives a two-dimensional schematic scenario showing the reconnection site and how jets are ejected upward and accelerated by a slingshot effect, where field lines make a whiplike movement. Cool material, trapped within a closed configuration, may be released along open field lines by a magnetic field disruption; recalling that cool plasma has been observed in the AR (see § 2), we surmise that this may be the origin of the EIT jets.

We can make a crude estimate of the energy fed into jets, assuming as typical parameters the values derived at the $\approx 1.7\ R_\odot$ distance where the UVCS slit was set. For a temperature $T_e \approx 10^5$ K, a density $n_e \approx 10^7$ cm^{-3}, a lifetime t, at $\approx 1.7\ R_\odot$ on the order of 30 minutes, a typical speed $v \approx 150$ km s^{-1}, and a diameter of jets of 100″, the gravitational, kinetic, and thermal energy add to a total of $\approx 2.1 \times 10^{28}$ ergs. Table 3 shows that the jet energy is mostly in the form of gravitational energy, while thermal energy plays a negligible role, amounting to $\approx 1/100$ of the gravitational energy.

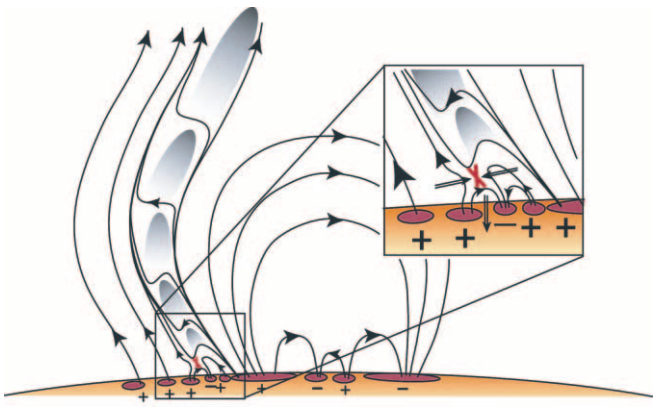

FIG. 15.— Cartoon representing the configuration where the 2003 May 25–27 jets occurred.

The above estimate does not include energy that possibly goes into energetic particles, as observed for the Wang et al. (2006) jets. As we said (see § 4), we do not expect to detect energetic particles in the present events, as they are on the east limb of the Sun; this may lead to an underestimate of their total energy.

Reconnection of a magnetic field B on the order of $B \approx 50$ G within a cube of side $L = 6000$ km can easily supply the jet energy. These representative values seem to be realistic in an AR: Bleybel et al. (2002) calculated the total energy of an eruptive AR where a long duration flare occurred, on 1995 October 14, and came up with a value of 8×10^{32} ergs. Should this be typical of ARs, recurrent events like those we are dealing with represent a negligible loss in the total AR energy budget.

We may try comparing the 2003 May jets with those analyzed over the past few years. The Ko et al. (2005) work, mentioned in § 1, focuses on a jet that is different from the jets we analyzed in several aspects: UV line intensities are higher by factors 10–100, higher temperatures than those required by UV lines were present, abundances are 0.3 times their photospheric values, and blueshifts

TABLE 3

GRAVITATIONAL, KINETIC, AND THERMAL ENERGY IN JETS

Parameter	Value
E_{gr} (ergs)	1.9E28
E_{kin} (ergs).....	2.1E27
E_{th} (ergs)	1.5E26

and redshifted lines have been observed. LASCO images, however, did not yield any firm detection of the jet whose dynamical properties can be reproduced by a ballistic model. Ko et al. (2005) conclude that the characteristics of their jet comply with predictions from the magnetic reconnection models of Shimojo et al. (1996) and successive developments, where hot and cool material coexist and may be ejected as a consequence of reconnection between an emerging flux and an overlying, oblique field.

UV spectra of jets have been analyzed also by Dobrzycka et al. (2000, 2002, 2006). These jets, opposite to those analyzed here, occur in polar coronal holes and originate from reconnection between the dipolar field of bright points (BPs) and the open fields of the coronal hole where BPs occur. They are well correlated with EIT and LASCO events and have intensities similar to those we measured. These characteristics make the Dobrzycka et al. jets look similar to the present events. There may be subtle differences, however, between the two: the Dobrzycka et al. jets are seemingly well correlated with Fe XII EIT structures and, although the UVCS spectrum not always included the C III line, when it did include the appropriate range of wavelengths no C III line was observed (see Dobrzycka et al. 2002).

It is difficult for us to speculate on the association, or lack of association, between EIT Fe XII jets and the 2003 May He II jets. During the He II campaign, only a few EIT Fe XII images are acquired over a day. However, we speculate that little, if any, hot Fe XII plasma was associated with our jets. Analysis of EIT Fe XII images, acquired before the He II campaign started, shows very little evidence of Fe XII jets. We point out that this also holds true for the Bemporad et al. (2005) C III jets, which occurred within a streamer (and have been referred to as ''puffs'' in that paper); very few, if any, Fe XII jets could be observed when the He II campaign terminated. This is also confirmed by the absence of Si XII λ998.76 emission in the jet. The Si XII line, fairly visible in the streamer adjacent to the jet, maximizes at $T_e = 2.5 \times 10^6$ K, and it will also be observable at $T_e = 1.3 \times 10^6$ K. Fe XII λ1242.0 emission maximizes at $T_e = 1.3 \times 10^6$ K: hence if such a hot plasma was present we would be able to detect the Si XII line. We suggest, on the basis of the admittedly incomplete evidence we have, that there is a class of cool jets in which little, if any, hot plasma is ejected.

We may wonder how frequent jets, specifically cool jets, are. In the present sample, the frequency of occurrence of EIT He II jets (about 10 multiple events per day over 2003 May 25–27) is a lower limit to its real value because of the low cadence (every 12 minutes) of image acquisition. An even lower frequency of occurrence would be inferred from UVCS data because LASCO images bear evidence of EIT jets not detectable in UVCS spectra. Possibly, this discrepancy is due to projection effects: when jets do not lie on the plane of the sky, their true altitude is larger than it appears and their emission may be too weak to be detected. Analogously, in the fall 2002 *SOHO*-Sun-*Ulysses* quadrature campaign, when SUMER joined the campaign, Teriaca et al. (2004) found at least one jet not detected by UVCS, which was clearly seen in LASCO C2 field of view. In this case as well, SUMER spectra provided no evidence for jets plasmas at temperatures $\approx 10^6$ K.

Analogously to flares, which cover a large span of energies, jets appear to range from cool Hα surges to X-ray jets, and to the variety of UV jets discussed here and by other authors. They all seem to originate from reconnection events between a closed and an open field, and should narrow CMEs originate from (see § 1) expanding loops, they would not belong to the jet family. We expect that more observational and theoretical work needs to be done to put jets in a unified scenario and understand what dictates their properties (magnetic field strength, altitude where reconnection occurs, short-lived reconnection bursts or longer lasting reconnection) and what their role is in larger scale phenomena, such as solar wind and CMEs.

SOHO and *Ulysses* are missions of international cooperation between ESA and NASA. G. P. acknowledges support from the ASI/INAF contract I/035/05/0. S. T. S. acknowledges support of *Ulysses*/SWOOPS and the *Ulysses* project. The authors thank Yi-Ming Wang for providing the field line extrapolations that appear in Figure 14.

REFERENCES

Bemporad, A., Moore, R. T., Sterling, A., & Poletto, G. 2005, ApJ, 635, L189
Bemporad, A., Poletto, G., Suess, S. T., Ko, Y.-K., Schwadron, N. A., Elliott, H. A., & Raymond, J. C. 2006, ApJ, 638, 1110
Bleybel, A., Amari, T., van Driel-Gesztelyi, L. & Leka, K. D. 2002, A&A, 395, 685
Brueckner, G. E., et al. 1995, Sol. Phys., 162, 357
Delaboudinière, J.-P., et al. 1995, Sol. Phys., 162, 291
Dobrzycka, D., Cranmer, S. R., Raymond, J. C., Biesecker, D. A., & Gurman, J. B. 2002, ApJ, 565, 621
Dobrzycka, D., Raymond, J. C., Biesecker, D. A., Li, J., & Ciaravella, A. 2003, ApJ, 588, 586
Dobrzycka, D., Raymond, J. C., & Cranmer, S. R. 2000, ApJ, 538, 922
Dobrzycka, D., Raymond, J. C., DeLuca, E., Gurman, J. B., Fludra, A., & Biesecker, D. A. 2006, in Proc. *SOHO* 17: 10 Years of *SOHO* and Beyond, ed. H. Lacoste (ESA SP-617; CD-ROM; Noordwijk: ESA)
Feldman, U., Mandelbaum, P., Seely, J. F., Doschek, G. A., & Gursky, H. 1992, ApJS, 81, 387
Gibson, S. E., Fludra, A., Bagenal, F., Biesecker, D., Del Zanna, G., & Bromage, B. 1999, J. Geophys. Res., 104, 9691
Gilbert, H. R., Serex, E. C., Holzer, T. E., McQueen, R. M., & McIntosh, P. S. 2001, ApJ, 550, 1093
Guhathakurta, M., Fludra, A., Gibson, S. E., Biesecker, D., & Fisher, R. 1999, J. Geophys. Res., 104, 9801
Handy, B. N., et al. 1999, Sol. Phys., 187, 229
Harrison, R. A., et al. 1995, Sol. Phys., 162, 233
Ko, Y.-K., et al. 2005, ApJ, 623, 519
Kohl, J. L., et al. 1995, Sol. Phys., 162, 313
Li, X., Habbal, S. R., Kohl, J. L., & Noci, G. 1998, ApJ, 501, L133
Pick, M., Mason, G. M., Wang, Y.-M., Tan, C., & Wang, L. 2006, ApJ, 648, 1247
Reames, D. V. 2002, ApJ, 571, L63
Scherrer, P. H., et al. 1995, Sol. Phys., 162, 129
Shibata, K., Nozawa, S., & Mashimoto, R. 1992a, PASJ, 44, 265
Shibata, K., et al. 1992b, PASJ, 44, L173
Shimojo, M., Hashimoto, S., Shibata, K., Hirayama, T., Hudson, H. S., & Acton, L. W. 1996, PASJ, 48, 123
Suess, S. T., Poletto, G., Romoli, M., Neugebauer, M., Goldstein, B. E., & Simnett, G. 2000, J. Geophys. Res., 105, 25033
Teriaca, L., Curdt, W., & Poletto, G. 2004, in Proc. *SOHO* 13, Waves, Oscillations and Small-Scale Transient Events in the Solar Atmosphere, ed. H. Lacoste (ESA-SP 547; Noordwijk: ESA), 291
Tsuneta, S., et al. 1991, Sol. Phys., 136, 37
Wang, Y.-M., Pick, M., & Mason, G. M. 2006, ApJ, 639, 495
Wang, Y.-M., & Sheeley, N. R., Jr. 2002, ApJ, 575, 542
Wang, Y.-M., et al. 1998, ApJ, 508, 899